

Model-Based Normalization for Iterative 3D PET Image Reconstruction

‡B Bai, ‡Q Li, ‡E Asma, †Y C Tai, †A Chatziioannou, ‡R M Leahy

‡Signal and Image Processing Institute, Univ. of Southern California, Los Angeles, CA 90089

†Crump Institute for Molecular Imaging, University of California, Los Angeles CA 90095

Abstract— We describe a method for normalization in 3D PET for use with model-based image reconstruction methods. This approach is an extension of previous factored normalization methods in which we include separate factors for detector sensitivity, geometric response, block effects and deadtime. Since our MAP reconstruction approach already models some of the geometric factors in the forward projection, the normalization factors must be modified to account only for effects not already included in the model. We describe a maximum likelihood based approach to joint estimation of the normalization factors which we apply to data from a planar source. We then compute block-wise and block-profile deadtime correction factors using singles and coincidence data, respectively, from a multiframe cylindrical source. We have applied this method for reconstruction of data from the LSO Concorde P4 microPET scanner. Preliminary results compare favorably with those obtained using normalization based directly on cylindrical phantom measurements.

Keywords— 3D PET, Normalization, Image Reconstruction

I. INTRODUCTION

Accurate normalization is essential for accurate quantitative 3D PET. Inaccuracies in normalization factors can result in artifacts, poor uniformity, and increased noise in the reconstructed images. Traditional solutions to the normalization problem include direct and component-based methods. In direct methods, a known source of activity is scanned, then the normalization factors are estimated as the ratio between the ideal number of coincidences and those actually measured [1]. The main problem with this method is that it requires that a very large number of counts be detected to achieve acceptable statistical accuracy for each line or response (LOR). To maximize the number of counts over all LORs, direct approaches typically use a uniform cylindrical source. Unfortunately, this introduces its own problems since the observation model is complicated by a substantial scatter fraction.

Hoffman [2] proposed a component-based method which divides the normalization factors into detector efficiency and spatial distortion correction, which accounts for the radial mispositioning due to the geometry of the scanner. This model reduces the number of counts required by reducing the degrees of freedom in the normalization model so that the normalization factors are computed by averaging over multiple LORs. Casey [3] and Badawi [4] extended

this concept to develop sophisticated models accounting for a wide variety of factors affecting detection efficiency. Casey’s normalization model includes intrinsic detector efficiency, geometric factors, crystal interference and dead-time factors, Badawi added time-alignment factors and a count-dependent block-profile to this model.

These models are complex and involve the sequential estimation of multiple types of normalization factors, often from different data sets. This can lead to inconsistent estimates since the normalization models are multiplicative. While optimal estimation of individual components, e.g. the detector efficiencies [1], [5], have previously been investigated, joint estimation of all factors in the component-based models has not, to the best of our knowledge, previously been described. Here we present a unified model in which all factors are estimated simultaneously within a maximum likelihood framework. This model is specifically matched to the model-based Maximum A-Posteriori (MAP) reconstruction methods [6]. The combination of our previously described system model with matched normalization allows us to explicitly account for the imperfections in the line-integral model using an accurate physical and statistical model for coincidence detection. In this way we build on our previous model, which included effects of detector solid angle, photon pair non-colinearity and intercrystal scatter and penetration, to also include effects arising from the block design, individual detector efficiencies, geometric effects, and deadtime.

II. METHODS

A. Normalization within a statistical image reconstruction framework

We have developed a MAP estimation algorithm to reconstruct 3D PET images [6]. In this approach, the data are modeled as:

$$\bar{\mathbf{y}} = \mathbf{P}\mathbf{x} + \bar{\mathbf{r}} + \bar{\mathbf{s}} \quad (1)$$

where $\bar{\mathbf{y}}$ is the mean of the data, \mathbf{x} is the source distribution, $\bar{\mathbf{r}}$ is the mean of the randoms, and $\bar{\mathbf{s}}$ is the mean of the scattered events. \mathbf{P} is the system matrix describing the probability that an event is detected, which we factor as:

$$\mathbf{P} = \mathbf{P}_{\text{norm}}\mathbf{P}_{\text{blur}}\mathbf{P}_{\text{attn}}\mathbf{P}_{\text{geom}} \quad (2)$$

where \mathbf{P}_{geom} is the geometric projection matrix describing the probability that a photon pair reaches the front faces of a detector pair in the absence of attenuation and assuming perfect photon pair colinearity. \mathbf{P}_{blur} models photon

pair non-colinearity, intercrystal scatter and crystal penetration, \mathbf{P}_{attn} contains attenuation correction factors for each detector pair, and \mathbf{P}_{norm} is a diagonal matrix containing the normalization factors.

The effects of solid angle variation at the detectors relative to the position of each voxel along a line of response and the angle between the detector surface and the LOR are accounted for in \mathbf{P}_{geom} . Similarly, the effects of crystal penetration that result in mispositioning of events towards the edge of the field of view is included in \mathbf{P}_{blur} . Consequently, these need not be included in the normalization factors as they are in previous factored methods [3]. Nevertheless, there are geometric factors that are not accounted for in (2) that we include in our normalization model as described below.

The normalization model we use here is that the diagonal matrix \mathbf{P}_{norm} has elements

$$\mathbf{P}_{\text{norm}}(i, i) = \varepsilon_{d1^i} \varepsilon_{d2^i} g(l, j, k)^i \tau_{b1^i, b2^i} d_{d1^i} d_{d2^i} \quad (3)$$

where we have used i to index the LORs. The specific detectors forming this LOR are denoted $d1^i$ and $d2^i$, and $b1^i$ and $b2^i$ are the blocks containing these detectors. The components of this model are as follows:

Geometric factors $g(l, j, k)^i$: $(l, j, k)^i$ represent, respectively the radial position l , the view angle j , and the sinogram index k , associated with LOR i . The sensitivity of each LOR is a function of the position of the two detectors in the block and the distance of the LOR from the center of the field of view of the scanner. Our geometric factor essentially combines the geometric and block-interference patterns of [3] into a single factor. Since the scanner is highly symmetric both axially and transaxially, many LORs are equivalent in these respects. The average number of LORs sharing the same block and radial positions is approximately 2.3×168 (the number of blocks in the Concorde scanner - 336 detectors for each of 32 rings in blocks of 8 by 8). Fig. 1 illustrates the symmetries of the LORs with respect to the blocks that we use in computing the normalization: each LOR can have up to an 8-fold symmetry with respect to a single block. This pattern then repeats every 8 detectors for an 8 by 8 block design.

Detector efficiency $\varepsilon_{d1^i}, \varepsilon_{d2^i}$: these quantities describe the intrinsic efficiencies of the two detectors forming the LOR. The total number of these factors is equal to the number of detectors.

Time-alignment factor $\tau_{b1^i, b2^i}$: The time alignment factor is based on the model proposed by Badawi [4] to account for differences in timing synchronization between different blocks. As the timing windows become misaligned between any pair of blocks, so the detection efficiency will drop. We can characterize the timing properties of each block by a single delay factor. The time-alignment factor for each LOR is then a function of the difference between the delay factors for the two blocks for that LOR. The form of this function can be determined experimentally by varying the timing between a pair of blocks. We have not yet performed this experiment so that in the results pre-

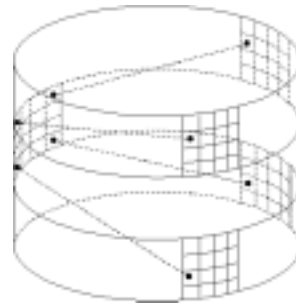


Fig. 1. The geometric factors are functions of the radial position of the LOR and the positions of the two detectors within their respective blocks. Illustrated here for a 4 by 4 block detector system is a four-fold symmetry in these factors. An additional two fold symmetry results from rotating and axially translating the LORs so that each of the four blocks on the right of the figure moves to the location of the left most block.

sented below we instead estimate directly a separate time-alignment factor for each pair of blocks.

Deadtime factor $d_{d1^i} d_{d2^i}$: the deadtime factors are estimated separately as described in Section II-C.

B. Normalization factor estimation

We compute the normalization factors from the previous section using a joint optimization procedure. This differs from the common practice of using rotating rod sources to compute geometric factors and cylinder data to compute geometric efficiencies [3], [4]. This provides self consistent estimates of the unknown parameters. Moreover, by basing the estimation on the model (1), the normalization is matched to the specific forward projection model that we subsequently apply during reconstruction. For the plane source used in our studies, scatter is minimal and we currently ignore scatter contributions. For the Concorde microPET scanner, data is initially collected in listmode format so that we can re-sort into simultaneous prompt and delayed event sinograms. Prior to computing the normalization factors, we use a Bayesian technique to estimate the mean of randoms from the separate randoms sinogram [7].

We model the measurements as Poisson using the model (1) to give the log likelihood:

$$L(\mathbf{P}_{\text{norm}}) = \sum_{i=1}^N y_i \log \{ \varepsilon_{d1^i} \varepsilon_{d2^i} g(l, j, k)^i \tau_{b1^i, b2^i} [\mathbf{P}\mathbf{x}]_i + \bar{\mathbf{r}}_i \} - \{ (\varepsilon_{d1^i} \varepsilon_{d2^i} g(l, j, k)^i \tau_{b1^i, b2^i}) [\mathbf{P}\mathbf{x}]_i + \bar{\mathbf{r}}_i \} \quad (4)$$

The source distribution \mathbf{x} is the known plane source. We estimate the parameters by maximizing $L(\mathbf{P}_{\text{norm}})$ using a grouped coordinate ascent method, updating each of the different factors in turn using steepest ascent with a Newton-Raphson line search. We find in practice that effective convergence is reached in 5 iterations with 3 sub-iterations of line search at each main iteration.

We assume for the purposes of computing the count-independent normalization factors, that the plane source is of sufficiently low activity that deadtime effects are minimal. This assumption is reasonable for the LSO detectors in the Concorde scanner for which deadtime factors are considerably lower than they would be for a BGO system.

Deadtime is affected by the properties of the PMT and detection electronics [4]. Rather than adopt the exponential model that was developed by Casey [3], we instead use an empirical quadratic correction method [4] which relates observed and true singles rates at each block by

$$\lambda_t = \frac{\lambda_a}{1 + \alpha\lambda_a + \beta\lambda_a^2} \quad (5)$$

where λ_t is the true singles rate, λ_a is the detected count rate, and α and β are experimentally determined parameters. We allow a separate deadtime calibration of this type for each detector block in the system, based on the measured singles rate for that detector block.

Block detectors also exhibit an additional deadtime effect, characterized by gradual mispositioning of events towards the middle of the block as the count rate increases [8], [4]. This mispositioning contributes to a count dependent variation of sensitivity across the detector blocks, which we report on below. Our results indicate that these variations are significant so that we include these factors in our deadtime correction.

Thus our overall deadtime model for each detector d_i , similar to that in [4], is the product of the mispositioning deadtime $d_{mp}(d_i)$ and PMT and electronics deadtime $d_{pp}(b_i)$:

$$d_{d_i} = d_{mp}(b_i) \times d_{pp}(d_i) \quad (6)$$

where b_i is the block containing detector d_i . The deadtime correction factor for each LOR is then the product of the factors for the two detectors forming the LOR.

We estimate the factors $d_{mp}(b_i)$ by observing the singles rate at each detector block over a series of I frames, taken as an F-18 source decays over the expected range of activities for the scanner. Since the LSO detectors have a natural background activity, we model the true activity at the block as

$$\lambda(t) = Ae^{-\phi t} + C \quad (7)$$

where A is the initial singles rate, ϕ is the decay constant, and C is the background activity. Integrating this activity over the duration of each frame from time t_i to t_{i+T} and applying the deadtime model (5) we obtain the series of equations:

$$\frac{A}{-\phi T} \left[(e^{-\phi(t_i+T)} - e^{-\phi t_i}) \right] + C = \frac{\lambda_{a,i}}{1 + \alpha\lambda_{a,i} + \beta\lambda_{a,i}^2} \quad (8)$$

for $i = 1, \dots, I$ where $\lambda_{a,i}$ is the observed total singles rate at the i th block and α and β are the constants to be estimated. This set of equations are solved using nonlinear least squares to obtain a separate pair of parameters for each detector block. The mispositioning deadtime parameters were computed as described in [5].

A. Plane source experiments

Using the method described above, we estimated normalization factors for the Concorde MicroSystems P4 microPET scanner. We acquired data for a 90x200x2mm plane source of volume 38cc filled with 700 μ Ci of FDG. The first frame was collected for 20 minutes, the source was then rotated by 30 degree increments, with frame durations adjusted to achieve approximately equal counts in each frame. We windowed each sinogram to take only lines of response within $\pm 15^\circ$ of the normal to the plane. The set of six windowed sinograms were then used to estimate the normalization factors.

B. Deadtime experiments

A 221.6cc cylinder, diameter 5cm and length 15.5 cm, containing 4.80 mCi F-18 solution was scanned for 19 frames. The duration of each frame was 600s with each new frame starting 0.5 half-lives after the previous one. The average singles rate for the first frame for each block was 1.43×10^5 , the average singles rate for the last frame was 827 (which was largely due to background radiation from LSO). The listmode format from the scanner allows us to acquire separate prompt and delayed sinograms and the singles rates for each individual detector block. These data were used to compute the deadtime factors.

C. Cylinder uniformity

Using the new normalization factors, we reconstructed a 5 cm diameter uniform cylinder. For comparison, we used a normalization file generated directly from a 2 hour duration frame from a uniform cylinder.

IV. RESULTS

Shown in Fig 2 are the block-wise and block-profile components of the deadtime correction factors. Fig 2(a) shows the excellent count-rate linearity for the LSO block detectors in the scanner over a wide activity range. The block-profile results indicate that these factors introduce significant count-dependent variations in sensitivity as a function of position in the block which should be included as part of the normalization process.

In Figs. 3 and 4 we show the effects of applying the model-based normalization procedure described here to reconstruction of a uniform cylinder compared to direct normalization based on a uniform cylinder. In both cases, the images were reconstructed using 30 MAP iterations with all algorithm parameters otherwise equal. Fig. 3 shows a single transaxial plane, and a profile through this plane, from the reconstructed cylinder. These results indicate some improvement in transaxial uniformity and a small reduction in noise. The latter observation was verified by computing region of interest variances which found a reduction in the percent standard deviation to mean ratio from 20% to 18%. The rise in activity towards the edge of the field of view that can be seen in both profiles is caused by the presence of scatter in the sinograms which was not corrected for in

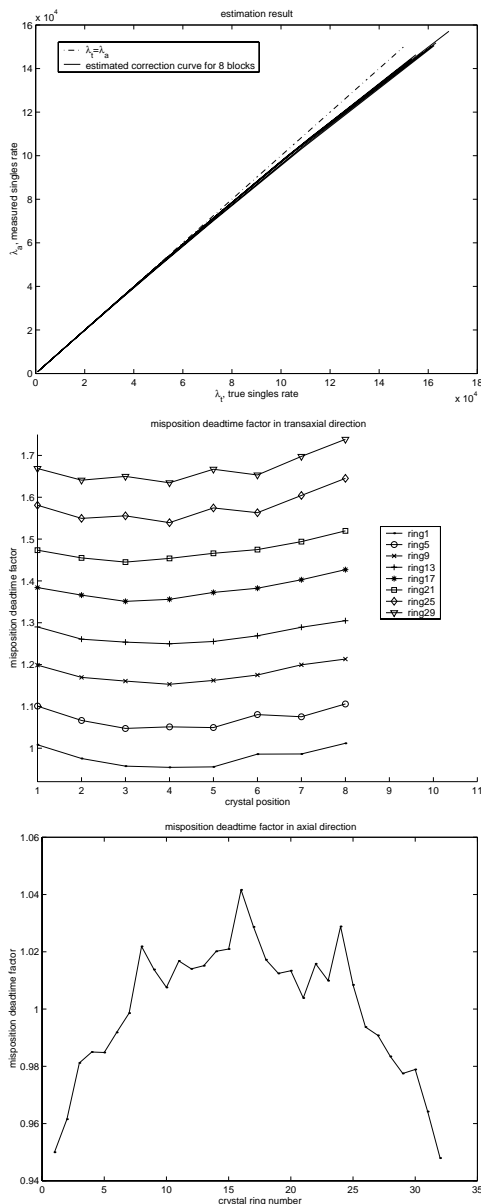


Fig. 2. Deadtime correction factors: (a) results from fitting the quadratic deadtime model to singles data from a 4.8mCi cylinder; shown are the measured vs. true singles rates for 8 different block detectors; (b) transaxial block profile factors computed from coincidence data for a measured singles rate of 20K for 8 different detector rings; (c) axial block profile from same data as (b).

these studies. Fig. 4 shows the axial uniformity as the total activity in each of the 63 reconstructed slices. Apart from over-correction in the first few planes, the model-based normalization produces improved axial uniformity compared to the direct normalization method.

The preliminary results presented show encouraging, if small, improvements in image uniformity compared to a direct normalization procedure. Further improvements should be realized as we refine our model. In order to compute the normalization factors in our approach, we must know the position of the plane source relative to the sinogram space. Currently we do this by comparing the measured plane source sinograms with the forward projection

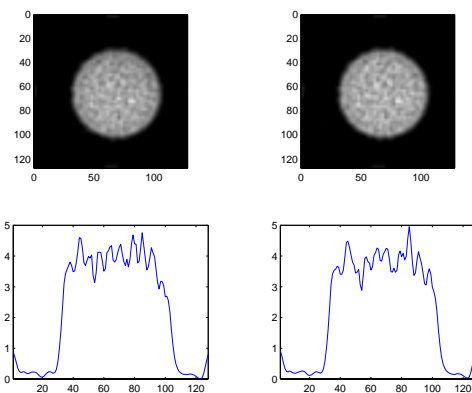


Fig. 3. Central plane of reconstructed cylinder. Left: model-based normalization; right: direct normalization.

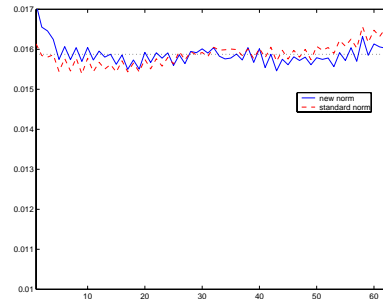


Fig. 4. Axial profiles of reconstructed cylinder using model-based and direct normalization.

of a simulated plane source, whose angle is adjusted so that the two sinograms match. Our procedure for performing this matching needs further refinement. We will also modify the time-alignment factor parameterization as we describe in Section II-A. Finally, we will include compensation for scatter to perform a full quantitative evaluation.

REFERENCES

- [1] M. Defrise, D. W. Townsend, D. Bailey, A. Geissbuhler, C. Michel and T. Jones: A normalization technique for 3D PET data. *Phys. Med. Biol.* **36**, 1991, 939–952
- [2] E. J. Hoffman, T. M. Guerrero, G. Germano, W. M. Digby, and M. Dahlbom: PET system calibrations and corrections for quantitative and spatially accurate images. *IEEE Trans. Nucl. Sci.* **33**, 1989, 1108–1112
- [3] Casey M. E., Gadagkar H. and Newport D.: A component based method for normalization in volume PET. *Proc. 3rd Int. Meeting on Fully Three-Dimensional Image Reconstruction in Radiology and Nuclear Medicine*, 1995, 67–71
- [4] R.D.Badawi, P. K. Marsden: Developments in component-based normalization for 3D PET. *Phys. Med. Biol.* **44**, 1999, 571–594
- [5] R.D.Badawi: Aspects of optimisation and quantification in three-dimensional Positron Emission Tomography. Ph.D thesis, University of London
- [6] J. Qi, R. M. Leahy, S. R. Cherry, A. Chatzioannou and T. H. Farquhar: High resolution 3D Bayesian image reconstruction using the microPET small-animal scanner. *Phys. in Med. Biol.* **43**, 1998, 1001–1013
- [7] E. U. Mumcuoglu, R. M. Leahy, S. R. Cherry, and Z. Zhou: Fast Gradient-Based Methods for Bayesian Reconstruction of Transmission and Emission PET Images. *IEEE Trans. Med. Imag.* **13**, 1994, 687–701
- [8] G. Germano, E. J. Hoffman: A study of data loss and mispositioning due to pileup in 2-D detectors in PET. *IEEE Trans. Nucl. Sci.* **37** 1990, 671–675.